EMD-Based Intelligent Crack Detection in Freight Railway Axles

A. Bustos[1](✉), H. Rubio[2], C. Castejon[2], and J. C. Garcia-Prada[1]

[1] MAQLAB Research Group, Department of Mechanics, UNED, C/ Juan del Rosal, 12, 28040 Madrid, Spain
albustos@ing.uc3m.es

[2] MAQLAB Research Group, Department of Mechanical Engineering, Universidad Carlos III de Madrid, Av. de la Universidad, 30, 28911 Leganes, Madrid, Spain

Abstract. The failure of railway axles can lead to catastrophic accidents, with the human and economic consequences that this entails. The vibratory performance of a freight train bogie is studied in this work aiming to identify the defects induced in the wheelset. The defects are generated mechanically with four severity levels. The bogie is tested in a roller rig test bench and vibration signals are recorded from sensors placed in the axle boxes of the wheelset. These signals are decomposed into several sub-signals using the Empirical Mode Decomposition. Then, the spectral power of these sub-signals is used as input for a Feedforward Neural Network to classify the vibration signals according to the defect level. The results show that the trained network can accurately identify the presence or absence of wheelset defects and their severity.

Keywords: Empirical Mode Decomposition · Feedforward Neural Network · Condition identification

1 Introduction

Increasing the reliability and availability of rolling stock is a key point to success in the competitive rail market and, also, an opportunity to reduce derailments, which occur more frequently in freight trains than in passenger trains [1]. But this strategy needs a good maintenance system able to detect failures on the rolling stock before an incident occurs.

Vibration analysis is one of the most used techniques for studying the condition of rolling stock, as it can detect several types of defects in components such as bearings [2], springs [3], wheel flats [4] or axle cracks [5]. One of the techniques usually applied to vibration signals is the Empirical Mode Decomposition (EMD), proposed by Huang et al. [6], which has proved to be an effective method to detect faults in bogies [7], wheelsets [8], and even in tracks [9].

M. Okada (Ed.): IFToMM WC 2023, MMS 149, pp. 815–825, 2024.
https://doi.org/10.1007/978-3-031-45709-8_79

In the current Industry 4.0 context [10], Artificial Neural Networks (ANNs) play a relevant role in the automatization of maintenance and fault identification. ANNs have been successfully applied for the identification of faults in bogies [11] and wheelsets [7, 12].

In this work, the dynamic behaviour of a freight train bogie with known axle defects is studied to train an ANN able to identify the axle's health condition. To that end, a freight bogie is equipped with a measurement system and tested in a roller test rig.

2 Experimental System

The tests were performed in a laboratory over a freight bogie, as shown in Fig. 1. The bogie is of type Y-21 Cse and is installed on a roller test rig that is composed of a rolling system, a loading system and a measurement system.

The maximum axle load of the Y-21 Cse bogie is 20 tons (this includes the own weight of the bogie) and the maximum speed is 100 km/h. The distance between axles is 2000 mm and the track gauge is 1668 mm. The nominal diameter of the wheels is 920 mm when new.

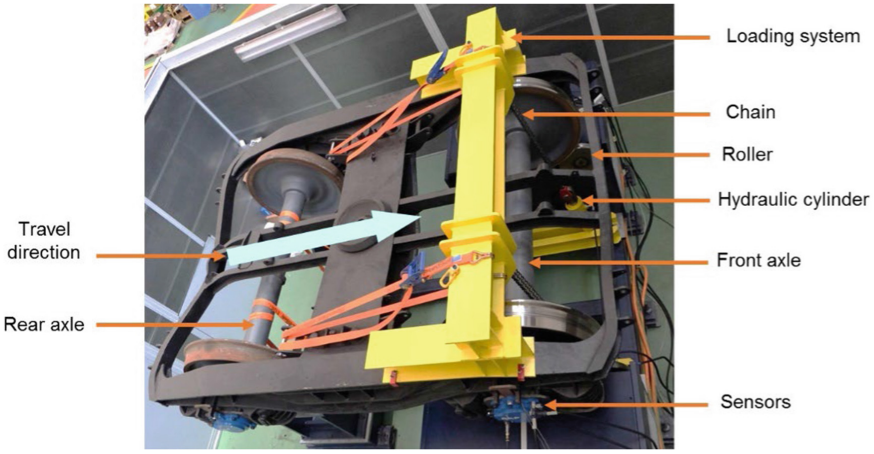

Fig. 1. Experimental system.

The front axle of the bogie rests in four steel rollers distributed in pairs. One roller of each pair is moved by an electric motor, being the two motors controlled electronically to rotate at the same speed and direction. The other two rollers are pulled by the wheel. The power transmitted to the rolling system allows the movement of the bogie wheels up to an equivalent speed of 80 km/h. The rotating direction of the wheels is established by the rotating direction of the rollers.

The rear axle of the bogie is fastened to the test rig foundation using slings, so the rear wheels are pressed down to a fixed rail section.

The nominal diameter of the four rollers of the test rig is 350 mm and the rolling surface has a UIC 60 profile with an inclination of 2.5°.

The loading system is composed of two hydraulic cylinders that pull down a steel frame (in yellow in Fig. 1) by using two double chains. This way, the bogie is pressed against the rollers and the contact between the wheels and the rollers is assured. The loading system is designed in a way that the pull force is applied directly to the loaded axle.

The accelerations on the axle boxes and the wheel speed are acquired and preprocessed by two IMx-R units which convert analogue signals to digital signals and store them in a computer.

Six uniaxial accelerometers are installed on the two axle boxes of the front wheelset, three on each side. The accelerometers are placed at the same point and oriented in the three space directions: longitudinal, axial and vertical directions. The technical characteristics of the accelerometers are specified in Table 1.

Table 1. Accelerometer technical characteristics.

Characteristic	SI
Sensitivity	10.2 mV/(m/s^2)
Measurement range	$\pm$ 490 m/s^2
Frequency range ($\pm$ 3 dB)	0.52 Hz to 8 kHz
Temperature range	-54 to $+$ 121 °C
Size (Length $\times$ Width x Height)	41.9 $\times$ 18.8 $\times$ 21.5 mm

The failure of the wheelset is simulated by cutting the axle with a circular saw to create a transversal crack in the centre of the wheelset (see Fig. 2). Four wheelset conditions are established based on the crack depth *e*, which is defined as seen on Fig. 2. These conditions are named d0, d1, d2 and d3 according to the values of the crack depth that are shown in Table 2. The sampling parameters used for acquiring the vibration signals are detailed in Table 3.

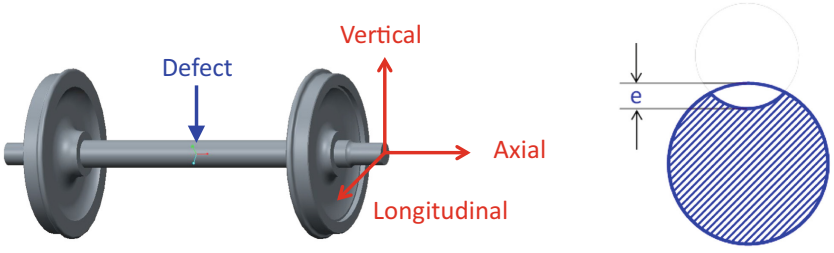

Fig. 2. Location (left) and shape and depth (right) of the defect.

Table 2. Crack depths.

Wheelset condition	Crack depth e (mm)
d0 (healthy wheelset)	0
d1	5.7
d2	10.9
d3	15

Table 3. Parameters of the signals measured.

Sampling frequency (Hz)	Acquisition time for each signal (s)	Number of points
12800	1.28	16384 (2^{14})

3 Signal Processing

In this work, a combination of EMD [6] and a Feedforward Neural Network (FNN) [13] is proposed for identifying the condition of the wheelset. To achieve this goal, the first step is the extraction of the first six Intrinsic Mode Functions (IMF). This task is carried out by using the algorithm proposed by Rilling [14]. As a result of the algorithm, the original signal x(t) can be reconstructed from the addition of a set of N_E components c_i and a residue r_N.

$$x(\mathrm{t}) = \sum_{i=1}^{N_E} c_i(t) + r_N(t) \tag{1}$$

Then, the power spectral density of the extracted IMF is obtained from Eq. (2), where Δt is the sample time, N is the number of data points in the signal, and $X(f)$ is the Fourier transform of the signal. Then, the signal's spectral power is computed. Therefore, we obtain six spectral power values for each signal that are used as input for the neural network.

$$S(f) = \frac{\Delta T}{N} |X(f)|^2 \tag{2}$$

An FNN is used for classifying the signals according to the wheelset condition. Therefore, the signals will be classified into four groups named d0, d1, d2 and d3. The structure of the neural network is as follows: the first layer is an input layer, the second layer is a fully connected layer followed by an activation function and another fully connected layer, a softmax function is laid next and, finally, an output layer.

The softmax layer is intended to normalize the output of the neural network [15]. To do this with n values, it is needed to find a vector in which each element must be between 0 and 1 and the entire vector must sum to 1. The softmax function is defined as given in Eq. (3), where z_i are the inputs and k is the number of classes in the response

variable.

$$softmax(z)_i = \frac{\exp(z_i)}{\sum_{j=1}^{k} \exp(z_j)} \tag{3}$$

4 Results

To perform the tests, the loading system is set at 10 t, which is half the maximum axle load of the bogie and applied to the front axle (Fig. 1). The speed is established at 50 km/h (wheel rotating frequency 4.97 Hz). Vibration signals are acquired in these conditions in both directions: forward, which corresponds to the clockwise (cw) rotation of the right wheel, and backwards, which corresponds to the counterclockwise (ccw) rotation of the right wheel. The wheel diameter of the wheelset tested is 890 mm.

Vibrations were recorded in the three space directions, in both axle boxes, but we will only focus on vertical vibrations in this work. The left and right sides are defined following the travel direction shown in Fig. 1.

After applying the EMD to the recorded signals, six sub-signals called IMF are extracted from each signal (Fig. 3). Then, the PSD (Fig. 4) and the spectral powers of these sub-signals are obtained. These data are combined with the wheelset condition to create tables that work as the input for the neural network. In all cases, 80% of the data is used for training and the remaining 20% is used for testing.

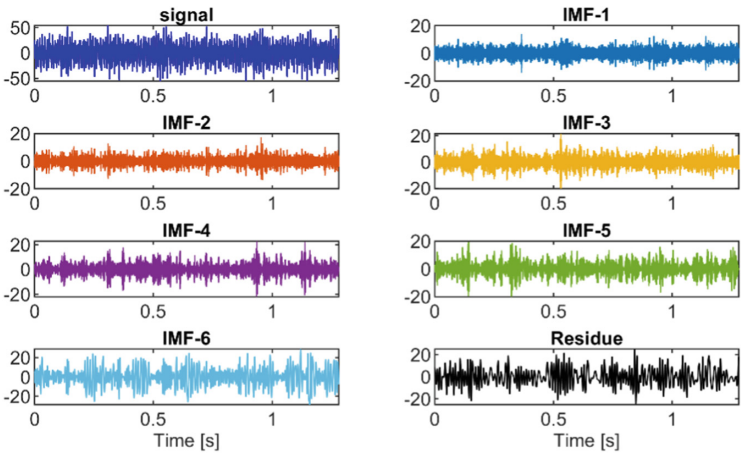

Fig. 3. Signal decomposition into six IMF and a residue.

The parameters of the FNN are varied in order to optimize the network and obtain the best results. This optimization is carried out using Bayesian methods and provides two possible solutions, depending on the criterion used. The "Bestpoint hyperparameters" criterion finds the set of hyperparameters that minimizes the upper confidence interval of the classification error objective model. The "Minimum error hyperparameters" finds

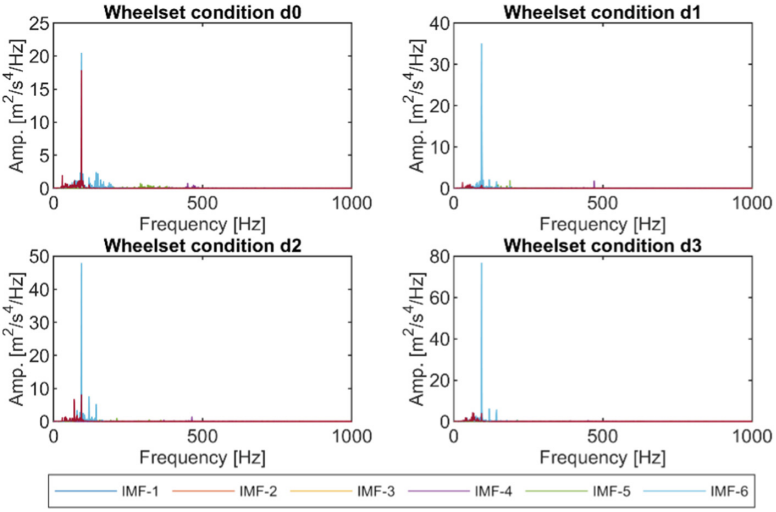

Fig. 4. PSD of the six IMF extracted from one signal in each wheelset condition.

the hyperparameters that minimize the observed classification error. Figure 5 shows the results of the optimization process, highlighting the points for the best hyperparameters and for the minimum error, which, in this case, are the same point. The final configuration of the network is shown in Table 4.

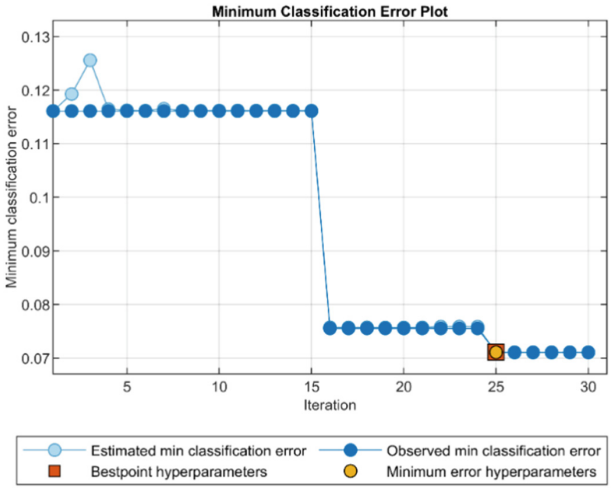

Fig. 5. Neural network optimization process.

This FNN configuration is employed to classify the recorded vibration signals grouped in five data sets that arise from the test settings: vibrations on the left side

in clockwise and counterclockwise directions, right side vibrations in clockwise and counterclockwise directions, and a combination of all data.

During the training process, the output of the network is validated, which leads to a validation accuracy rate. The accuracy rates of validation and testing for each data set are summarized in Table 5. As can be observed, the accuracy of the FNN tested is, in general, above 90%. The best results are obtained for the fourth data set, which is composed of the vibration signals recorded on the right side of the axle in ccw direction. In this case, the ANN classifies correctly 100% of the observations both in validation and testing. On the other hand, changing the rotating direction yields the worst results: the validation accuracy of RHS cw (right side, cw direction) is only 84.4%, increasing up to 94.55% when testing.

Figures 6, 7, 8, 9 and 10 show the ROC (Receiver Operating Characteristics) [16] curves obtained from the training and testing of the FNN with the data set of Table 5. These figures illustrate the accuracy achieved by identifying the four defect levels.

Regarding the LHS cw data set (see Fig. 6), it can be observed that the area under the curve (AUC), which is directly related to the accuracy of the model, is above 0.998 during the training phase. So it could classify correctly above 99.8% of data.

Table 4. Configuration of the FNN

Parameter	Value
Number of fully connected layers	2
Activation function	Tanh
Standardize data	Yes
Regularization strength (Lambda)	$2.5536 \cdot 10^{-6}$
First layer size	289
Second layer size	79

Table 5. Accuracy results

Data set	Validation accuracy (%)	Test accuracy (%)
LHS cw	98.65	96.36
LHS ccw	96.62	100
RHS cw	84.4	94.55
RHS ccw	100	100
LHS + RHS cw + ccw	93.65	95.18

The curve related to the testing phase reveals that the network can classify correctly all signals with defect levels 0 and 1, and has more difficulties in identifying signals within d2 or d3, although the ability to correctly classify data is above 99%.

Similar results are obtained when the wheelset is tested in the opposite rotating direction. The ROC curves of tests in the left side and ccw direction are shown in Fig. 7. The ability of the network to produce good scores during the training phase is above 99.3%. When tested, the network can classify correctly all the signals (100% accuracy) in one of the four defect levels defined.

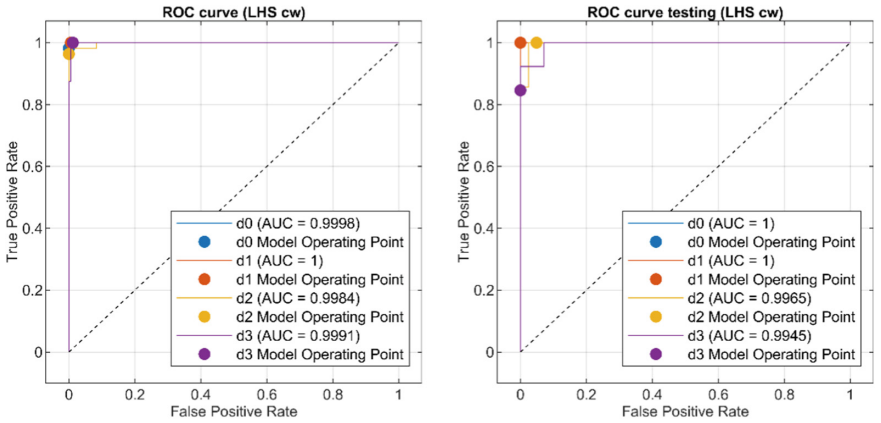

Fig. 6. ROC curves LHS clockwise data.

On the other hand, the classification of vibration signals recorded in the right hand of the bogie shows more differences between the rotating directions. Figure 8 illustrates the ROC curves corresponding to the right side of the axle and the clockwise direction. As can be seen, during the training stage, the network exhibits a good ability to identify adequately signals with defect levels d1 and d3. However, it shows some difficulties in identifying the signals that correspond to defect levels d0 and d2. In these cases, the AUC is just above 0.85. Results are better in the testing phase, where the ability to hit increases up to 90%.

The ability of the network to correctly classify the right side vibrations when the direction is set counterclockwise is 100%, as can be seen in Fig. 9. Network can classify correctly all the vibration signals both in the training phase and the testing phase. The AUC is 1 in all defect levels.

The last data set comprises the vibration signals recorded on both sides of the bogie (left and right) and both rotating directions (cw and ccw). The ROC curves (see Fig. 10) show good agreement between the predicted defect level and the actual defect level. The ability to hit is above 98% both in the training phase and the testing phase. Defect levels d1 and d3 are identified more precisely than defect levels d0 and d2.

5 Conclusions

This work uses a set of parameters based on the Empirical Mode Decomposition for feeding a Feedforward Neural Network with the aim of identifying the condition of a freight train bogie. Vibration signals are recorded in four different conditions: healthy

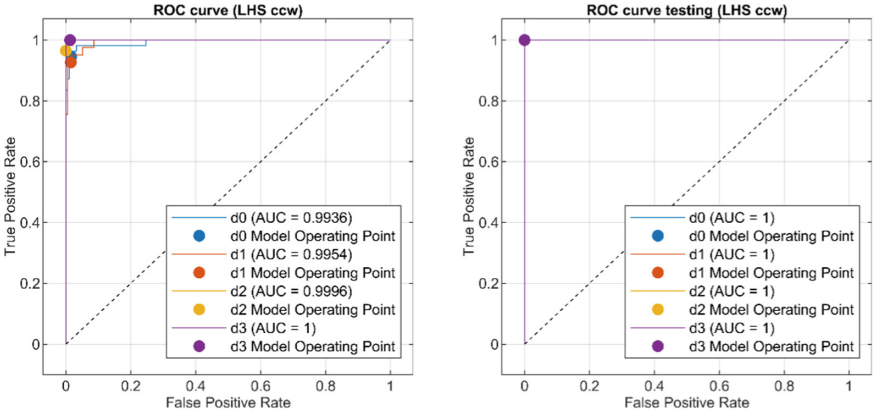

Fig. 7. ROC curves LHS counterclockwise data.

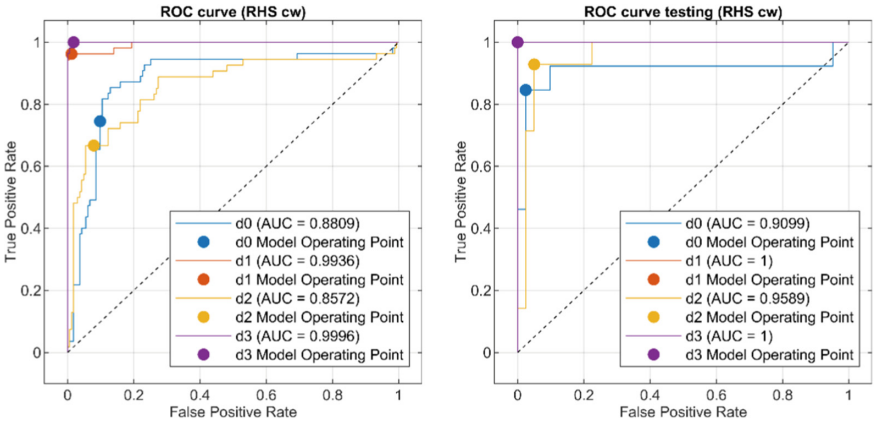

Fig. 8. ROC curves RHS clockwise data.

axle, slight defect, medium defect and severe defect, which are identified as defect levels d0, d1, d2 and d3, respectively.

The structure of the ANN is optimized by using Bayesian methods and, then, tested with five data sets coming from the tests performed over the bogie in a roller-rig test bench. Hence, vibration data are split according to the rotating direction of the axle and the side in which accelerations were measured.

In this work, 80% of the data is used for training and validating the ANN, and the remaining 20% is used for testing purposes. During the training and validating phase, the results show a good performance of the network in the identification of the wheelset condition, with accuracy rates above 90% in all cases except one, in which the precision is 84%. Accuracy rates are greater in the testing phase, with values above 94%. In several scenarios, the FNN correctly identifies the class of all vibration data (accuracy rate is

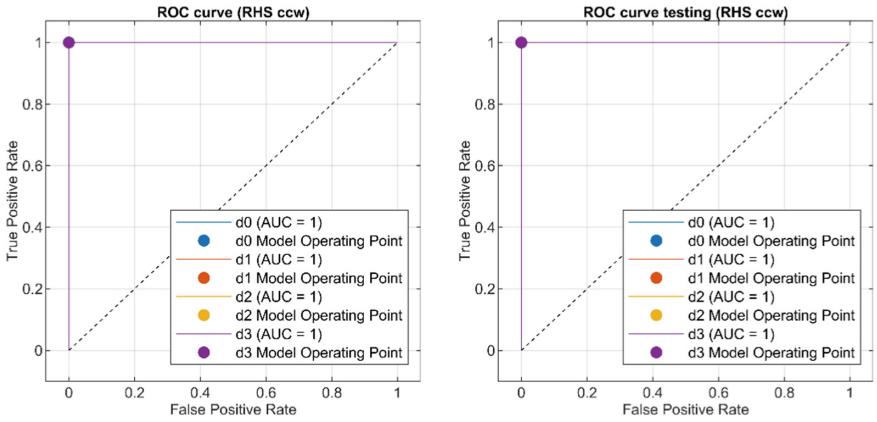

Fig. 9. ROC curves RHS counterclockwise data.

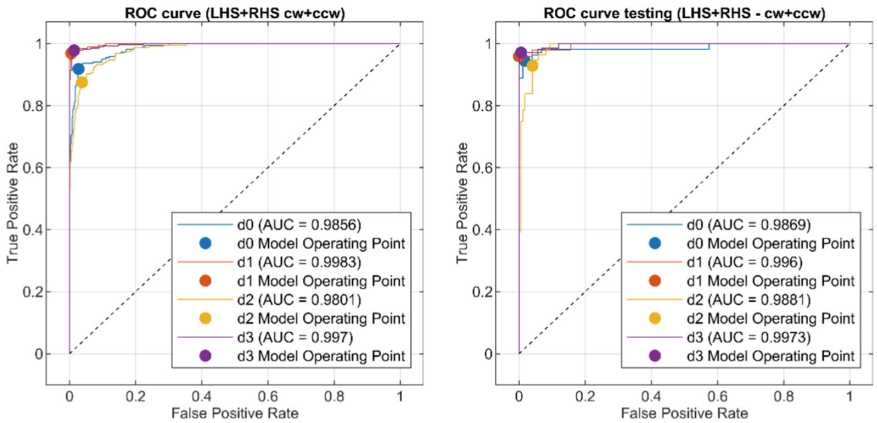

Fig. 10. ROC curves combining all data.

100%). Therefore, it can be concluded that the combination of EMD and the proposed FNN is a good strategy to identify the operating condition of the bogie.

Acknowledgements. This publication is part of the R&D&I project MC 4.0, funded by AEI/10.13039/501100011033 via sub-projects PID2020-116984RB-C21 and PID2020-116984RB-C22. It is also funded by UNED via the project 2023-ETSII-UNED-06.

References

1. Bernal, E., Spiryagin, M., Cole, C.: Onboard condition monitoring sensors, systems and techniques for freight railway vehicles: a review. IEEE Sensors J. **19**, 4–24 (2019). https://doi.org/10.1109/JSEN.2018.2875160

2. Li, Y., Liang, X., Chen, Y., Chen, Z., Lin, J.: Wheelset bearing fault detection using morphological signal and image analysis. Struct Control Health Monit. **27**, (2020). https://doi.org/10.1002/stc.2619
3. Li, C., Luo, S., Cole, C., Spiryagin, M.: Bolster spring fault detection strategy for heavy haul wagons. Veh. Syst. Dyn. **56**, 1604–1621 (2018). https://doi.org/10.1080/00423114.2017.1423090
4. Bernal, E., Spiryagin, M., Cole, C.: Wheel flat detectability for Y25 railway freight wagon using vehicle component acceleration signals. Vehicle Syst. Dynam. 1–21 (2019). https://doi.org/10.1080/00423114.2019.1657155
5. Bustos, A., Rubio, H., Meneses, J., Castejon, C., Garcia-Prada, J.C.: Crack detection in freight railway axles using power spectral density and empirical mode decomposition techniques. In: Uhl, T. (ed.) Advances in Mechanism and Machine Science. IFToMM WC 2019. pp. 3691–3701. Springer International Publishing, Cham (2019)
6. Huang, N.E., et al.: The empirical mode decomposition and the Hilbert spectrum for nonlinear and non-stationary time series analysis. Proc. Royal Soc. London A: Mathem. Phys. Eng. Sci. **454**, 903–995 (1998)
7. Huang, D., Li, S., Qin, N., Zhang, Y.: Fault diagnosis of high-speed train bogie based on the improved-CEEMDAN and 1-D CNN algorithms. IEEE Trans. Instrum. Meas. **70**, 1–11 (2021). https://doi.org/10.1109/TIM.2020.3047922
8. Rabah, A., Abdelhafid, K.: Rolling bearing fault diagnosis based on improved complete ensemble empirical mode of decomposition with adaptive noise combined with minimum entropy deconvolution. J. Vibroeng. **20**, 240–257 (2018). https://doi.org/10.21595/jve.2017.18762
9. Jauregui-Correa, J.C., Morales-Velazquez, L., Otremba, F., Hurtado-Hurtado, G.: Method for predicting dynamic loads for a health monitoring system for subway tracks. Front. Mech. Eng. **8**, 858424 (2022). https://doi.org/10.3389/fmech.2022.858424
10. Bustos, A., Rubio, H., Soriano-Heras, E., Castejon, C.: Methodology for the integration of a high-speed train in maintenance 4.0. J. Comput. Design Eng. **8**, 1605–1621 (2021). https://doi.org/10.1093/jcde/qwab064
11. Zhao, Y., Guo, Z.H., Yan, J.M.: Vibration signal analysis and fault diagnosis of bogies of the high-speed train based on deep neural networks. J VIBROENG. **19**, 2456–2474 (2017). https://doi.org/10.21595/jve.2017.17238
12. Krummenacher, G., Ong, C.S., Koller, S., Kobayashi, S., Buhmann, J.M.: Wheel defect detection with machine learning. IEEE Trans. Intell. Transport. Syst. **19**, 1176–1187 (2018). https://doi.org/10.1109/TITS.2017.2720721
13. Glorot, X., Bengio, Y.: Understanding the difficulty of training deep feedforward neural networks. In: Proceedings of the Thirteenth International Conference on Artificial Intelligence and Statistics. pp. 249–256. JMLR Workshop and Conference Proceedings (2010)
14. Rilling, G., Flandrin, P., Gonçalves, P., Lilly, J.M.: Bivariate empirical mode decomposition. IEEE Signal Process. Lett. **14**, 936–939 (2007). https://doi.org/10.1109/LSP.2007.904710
15. Goodfellow, I., Bengio, Y., Courville, A.: In: Deep Learning. MIT Press (2016)
16. Fawcett, T.: ROC graphs: notes and practical considerations for researchers. Mach. Learn. **31**, 1–38 (2004)